Construction and *in vitro* digestibility evaluation of a novel human milk fat substitute rich in structured triglycerides

Guibing ZENG[1,2,3], Wenran TIAN[1,2,3], Zheling ZENG[1,2,3*] (iD), Xianghui YAN[1,2,3], Ping YU[1,2,3*], Deming GONG[4], Jun WANG[2,3]

Abstract

The infants who cannot be breastfeed need to obtain energy and nutrition from other sources, such as formula. In this study, a human milk fat substitute (HMFS) rich in structured triglycerides (STG) and with a variety of fatty acids was prepared by one-step transesterification reaction. The optimum conditions for the lipase-catalyzed transesterification between basa catfish oil solid fraction, *Cinnamomum camphora* seed kernel oil, linseed oil, microbial oil and algae oil were studied and the *in vitro* digestibility of the constructed HMFS was investigated. Under the optimal conditions, the obtained HMFS contained 58.86% STG and 39.73% sn-2 palmitic acid (PA). Fatty acid composition analysis showed that HMFS was composed of capric acid (Ca), lauric acid (La), oleic acid (O), linoleic acid (L), linolenic acid (Ln), arachidonic acid (ARA) and docosahexaenoic acid (DHA). LC-MS/MS analysis found that 142 new triglycerides were generated, such as Ca-P-ARA, Ca-P-Ln, La-P-ARA, La-P-L and P-O-ARA. Moreover, compared with physical mixture (PM), HMFS had better melting and crystallization temperature and the fatty acid release rate of HMFS was significantly improved. These results suggested that HMFS may have a great application in infant food as a nutritional ingredient.

Keywords: human milk fat substitute; transesterification; structured triglycerides; *in vitro* digestibility.

Practical Application: A novel STG-rich HMFS was obtained for the first time through one-step transesterification reaction, which not only guaranteed the content of sn-2 PA, but also coordinated the composition of various fatty acids (C6:0 - C22:6).

1 Introduction

It is universally acknowledged that the ideal food for infants is human milk, which provides infants with almost all energy and nutrient for the first four to six months of life (Gahroui et al., 2022; Wei et al., 2019). Human milk fat (HMF) accounts for 3-5% of human milk and consist of approximately 98% triglycerides (TAG), which could provide around 50% infant's calories (Zou et al., 2016a). As one of the most complex natural lipid mixtures, HMF has an unique fatty acid composition, distribution, and numerous complex lipids. There are more than 50% palmitic acid (PA) at sn-2 position of TAG, and other fatty acids including long chain fatty acids (LCFAs), such as oleic acid (O), linoleic acid (L), arachidonic acid (ARA), docosahexaenoic acid (DHA) and linolenic acid (Ln), and medium chain fatty acids (MCFAs), such as capric acid and lauric acid, are mainly located at the sn-1, 3 positions of TAG (Zou et al., 2016b). The unique TAG structure of HMF is associated with digestion, absorption, and metabolism of fats and nutrients in infants. It was reported that more than 60% sn-2 fatty acids (mainly PA) were remained after digestion, which could improve the absorption and utilization of essential fatty acids and calcium to prevent infant constipation (Wang et al., 2021). However, for a variety of reasons, many infants cannot be breastfed, in which case the infants require other sources of energy and nutrition, such as infant formula.

Human milk fat substitute (HMFS) is one kind of lipid product produced by imitating the fatty acid composition and TAG structure of HMF, and is widely used in infant formula. However, there is an obvious difference between the sn-2 fatty acid composition and TAG structure of commercial infant formula and HMF (Yuan et al., 2019). In comparison with HMF, the sn-2 PA content in commercial infant formula is still lower (Sun et al., 2018). Moreover, MCFAs mainly exist together with LCFAs as structured lipids in HMF, which is rarely present in infant formula (Yuan et al., 2019). Therefore, it is necessary to make TAG and fatty acid composition similar to HMF and, simultaneously, with high content of sn-2 PA when HMFS is produced. In recent years, many researches have been done to prepare HMFS similar to HMF by lipase-catalyzed transesterification and/or physical blending. For example, Zou et al. (2016a) prepared 1,3-dioleoyl-2-palmitoylglycerol (OPO)-rich HMFS by Lipozyme RM IM-catalyzed acidolysis of basa catfish oil (solid fraction) with oleic acid containing high content of sn-2 PA (57.80%). Wang et al. (2021) developed a physical blending model to

prepare HMFS rich in 1-oleoyl-2-palmitoyl-3-linoleoylglycerol (OPL), and the contents of OPL and sn-2 PA in the synthesized OPL product were 47.93% and 87.90%, respectively. However, to our knowledge, these studies mainly focused on the major TAG structures (OPO and OPL) and sn-2 PA content in HMFS. There are limited information on the consideration of position and content of MCFAs in TAG. MCFAs are important source of energy for infants with the immature digestive system. This is because MCFAs can enter the mitochondria independently of the carnitine transfer system, which allows them to be quickly oxidized instead of accumulating in the body (Fu et al., 2015). In addition, MCFAs possess antibacterial activity, which may impact the establishment of infant's intestinal flora and relevant immunity (Nejrup et al., 2017).

In order to balance the contents of various fatty acids, different oil sources have been screened. The solid fraction of basa catfish oil (BCO) was found to have high sn-2 PA and low total PA content (Yuan et al., 2020). *Cinnamomum camphora* seed kernel oil (CCSKO) is an excellent source of MCFAs, with 51.49% capric acid (Ca) and 40.08% lauric acid (Fu et al., 2016). Linseed oil (LO) is a good source of L and Ln. Furthermore, microbial oil (MO) and algae oil (AO) have high contents of ARA and DHA. These oils could be used as starting materials for HMFS production. In order to obtain the ideal HMFS product with high sn-2 PA content and proper TAG structure, a structured triglycerides (STG) type HMFS product is recommended. STG can be obtained chemically or enzymatically. In recent years, enzymatic approaches are more preferable compared to chemical catalysts for the production of STG due to consumer spending trends favoring greater product safety (Zuin et al., 2022). In addition, enzymatic method can be applied under mild conditions, produce less by-product and easily recover catalysts which cannot be achieved through chemical methods. Enzymatic synthesis of STG can usually be achieved through acidolysis, esterification and transesterification (Zhang et al., 2021). Compared to acidolysis and esterification, transesterification is a preferred method of the synthesis of STG, as the levels of reaction by-products, such as free fatty acid, monoglyceride and diglyceride, were low and the yield of STG was relatively high.

The study aimed to construct HMFS based on the fatty acid content and TAG structure of HMF. Five different sources of oils were selected as raw materials. Lipase-catalyzed transesterification was used to achieve similar fatty acid composition to HMF and ensure high content of sn-2 PA. The optimum conditions of transesterification reaction (temperature, time and enzyme load) were investigated to maximize STG content. In addition, the *in vitro* simulated gastrointestinal digestion model was established to evaluate the digestibility of the prepared HMFS.

2 Materials and methods

2.1 Materials

BCO was provided by Heruikang (Vietnam) Edible Oil Co., Ltd. CCSKO was prepared by our group in the State Key Laboratory of Food Science and Technology, Nanchang University, China. LO was purchased from a local supermarket (Nanchang, China). AO and MO were provided by CABIO

Biotech (Wuhan) Co, Ltd. Six commercial immobilized lipases, NS 40086, Lipozyme 435, Novozyme 435, Lipozyme RM IM, Lipozyme TL IM and Lipozyme RM were purchased from Novozymes (Beijing, China). Thirty-seven fatty acid methyl esters (FAMEs) standards were purchased from Nu-Chek Prep Inc. (Elysian, MN, USA). All the solvents and reagents were of analytical or chromatographic grade.

2.2 Preparation of basa catfish oil solid fraction

The fractionation of basa catfish oil was conducted according to the method of Zou et al. (2016a) with slight modification. Briefly, basa catfish oil was heated at 80 ℃ for 40 min, and then cooled to 30 ℃ at a rate of 1 ℃/min. After kept at 30 ℃ for 24 h, the basa catfish oil solid fraction (BCO-SF) was separated from liquid oil by an aspirator filter pump.

2.3 Preparation of HMFS by lipase-catalyzed transesterification

Optimization of reaction conditions

Comparing the composition and distribution of HMF fatty acids in various countries and regions in the world (Wei et al., 2019), in HMF, capric acid and lauric acid make up 6-15% of all fatty acids, PA make up 20-25%, oleic acid make up 20-30%, linoleic acid make up 8-20%, and linolenic acid make up 1-4%, the content of ARA is 0.4-0.8%, and the content of DHA is 0.2-1%, depending on genetics, stage of lactation, and feeding regimens. Considering that the total amount of linoleic acid and linolenic acid accounts for about 20% of the total fatty acid, and excessive intake of linoleic acid induced adverse effects in healthy subjects (Janssen & Kiliaan, 2014), the total amount of linoleic acid and linolenic acid was set to about 20% with the ratio of 1:1.5. Studies have shown that high levels of ARA and DHA were beneficial to infant's nerve and vision development, and the content of ARA should not be lower than DHA (Colombo et al., 2017). The ratio of ARA and DHA was set to 1:1, and each accounted for 1% of the total fatty acid content. While considering the fatty acid composition, the content of PA at the sn-2 position should be as close as possible to the composition of HMF. According to the fatty acid composition of the oils, the mass ratio of the five oils (BCO-SF/CCSKO/LO/AO/MO = 0.615/0.061/0.249/0.043/0.032) was determined. The theoretical fatty acid composition of the five oils physical mixture was 10% for MCFAs, 8% for linoleic acid, 12% for linolenic acid, 1% for ARA, 1% for DHA, and 40% for sn-2 PA.

To obtain the optimal conditions of lipase-catalyzed transesterification reaction for the production of HMFS, the activities of six lipases, NS 40086, Lipozyme 435, Novozyme 435, Lipozyme RM IM, Lipozyme TL IM and Lipozyme RM were firstly evaluated. Then the optimal conditions (temperature, time and enzyme load) of the selected lipase were investigated.

A total of 100 g of BCO-SF, CCSKO, LO, AO and MO at the above mass ratio were mixed in a 250 mL three-necked flask, and then the lipase at 2, 4, 6, 8, 10, 12 or 14% (w/w) by the weight of total substrates was added. In the case of nitrogen as a protective gas, the enzymatic reaction was performed in an oil

bath at a stirring rate of 200 rpm at different temperatures (50, 55, 60, 65, 70 and 75 ºC) and times (0–10 h). Samples of 50 µL were withdrawn from the reaction system for analyses. After a given time, the lipase was removed by filtration. The filtrate and all samples were stored at -20 ºC for further analysis. All reactions were performed in triplicate.

Purification of reaction product

The crude HMFS (C-HMFS) was purified with 85% ethanol in a ratio of 1:20 (w/w) to remove the free fatty acids produced during the reaction. The extraction was repeated three times and the ethanol phase was removed. The final products were stored at -20 ºC for further analysis.

2.4 Determination of fatty acid composition

The fatty acid methyl esters (FAMEs) of sample were prepared using a previous method (MacHate et al., 2020; Zhao et al., 2019) with minor modifications. Briefly, approximately 25 mg oil sample was mixed with 2 mL of 0.5 mol/L NaOH-CH$_3$OH solution, and heated in a water bath at 65 ºC for 30 min. After cooled to room temperature, 2 mL of BF$_3$-CH$_3$OH solution (0.5 mol/L) was added and incubated at 70 ºC for 5 min. Subsequently, FAMEs were extracted with 2 mL of hexane and 4 mL of saturated NaCl solution. The mixture was vortexed for 2 min and stood to separate the organic and aqueous phases. The upper organic layer was filtered through an anhydrous sodium sulfate cartridge and 0.22 µm PTFE syringe membrane filter for gas chromatography (GC) analysis.

FAME samples were analyzed with an Agilent 7890B GC (Agilent Technologies Inc., Santa Clara, CA, USA) equipped with a flame ionization detector (FID) using a DB-23 fused silica capillary column (30 m x 0.25 mm x 0.25 µm). The injector and detector temperatures were set at 250 ºC and 280 ºC, respectively. The temperature program was as follows: holding at 50 ºC for 1 min, increasing to 175 ºC at a rate of 25 ºC/min, then increasing to 230 ºC at a rate of 3 ºC/min and holding for 10 min. The injection volume was 1 µL and N$_2$ was used as the carrier gas at a constant flow rate of 1 mL/min. The FAMEs in the samples were identified by comparing the retention times with those of standard FAME mixtures, and relative fatty acid content were calculated. All samples were analyzed in triplicate.

2.5 Determination of sn-2 fatty acid composition

A total of 30 mg oil was taken and isolated by thin layer chromatography plates with hexane: diethyl ether: acetic acid (70:30:1, v/v/v) (Zou et al., 2016a). The band corresponding to MAGs was scraped off to determine sn-2 fatty acid composition.

2.6 Determination of STG yield

The analysis of TAG species from BCO-SF, CCSKO, LO, AO, MO, PM, C-HMFS and HMFS was performed by the reversed-phase high performance liquid chromatography (RP-HPLC) on an Agilent 1260 Infinity HPLC system equipped with an Agilent 1260 evaporative light scanning detector (ELSD) (Agilent Technologies Inc., Santa Clara, CA, USA) and a Hypersil ODS

C18 analytical column (5 µm, 4.6 x 200 mm) (Elite Co., Dalian, China). Samples were diluted with isopropanol to 5 mg/mL and filtered by 0.22 µm PTFE syringe membrane filter. 5 µL filtered sample was injected into the HPLC system for analysis. The column temperature was set at 30 ºC. The mobile phase at a flow rate of 0.8 mL/min consisted of isopropanol (A) and acetonitrile (B). The gradient (0 min, 30% A and 30 min, 70% A) was used. The ELSD was set at 40 ºC and a gas flow rate was controlled at 1.6 mL/min. The STG yield was calculated using the following equation (Equation 1):

$$STG\ Yield\,(\%) = \frac{Weight\ of\ STG}{Weight\ of\ total\ reactants} \times 100$$

(1)

2.7 Determination of triglyceride structure

The lipid compositions under optimum interesterification reaction conditions were identified by using LC30 System (Shimadzu, Japan) equipped with a Hybrid Quadrupole-TOF Mass Spectrometer: Triple TOF 5600 + (AB Sciex, USA). Samples were diluted with isopropanol to 1 mg/mL and filtered by 0.22 µm PTFE syringe membrane filter. The analyte was separated with Hypersil ODS C18 column (5 µm, 200 mm × 4.6 mm; Elite, China) at 30 ºC. The sample injection volume was 10 µL. The mobile phase at a flow rate of 0.8 mL/min consisted of isopropanol (A) and acetonitrile (B). The gradient (0 min, 30% A and 40 min, 70% A) was used. Mass spectrometric analysis was conducted with atmospheric pressure chemical ionization (APCI) source under positive ion mode with the following conditions: curtain gas pressure, 40 psi; ion source gas 1, 55 psi; ion source gas 2, 55 psi; ion spray voltage, 5,500 V; ion source temperature, 550 ºC; collision energy, 10 eV; declustering potential, 80 V; scan range, 50-1,200 Da.

2.8 Fourier transform infrared (FT-IR) spectroscopy

The FT-IR spectra ranging from 4000 to 400 cm^{-1} of samples were obtained by Nicolet™ iS10 Fourier Infrared Spectrometer (Thermo Nicolet Co., USA). Each spectrum was scanned 64 times with a resolution of 4 cm^{-1} and scan speed of 1 cm/s (Uncu et al., 2019).

2.9 Characterization of thermal behavior

Samples (7-9 mg) was added into hermetic aluminum pans at room temperature and analyzed by a DSC250 (TA Instruments-Waters LLC, USA). The samples were equilibrated at -40 ºC for 5 min, and then heated to 80 ºC at a rate of 5 ºC/min. After equilibrated at 80 ºC for 5 min, the samples were cooled to -40 ºC at a rate of 5 ºC/min (Korma et al., 2018). Peak enthalpies and melting and crystallization temperatures were determined by the system software.

2.10 Preparation of emulsion

Soy lecithin was dissolved in ultra-pure water (0.2 mg/mL) as an emulsifier. The emulsion samples were prepared by dispersing 5 mL of oil phase (PM and HMFS) into 95 mL of water phase with a high-speed shear (T18, IKA, Germany) for

5 min (12,000 r/min). The freshly prepared emulsions were then subjected to the following studies.

2.11 In vitro digestion

The prepared emulsions were passed through a simulated *in vitro* gastrointestinal digestion model to monitor the fatty acid release rate (Souza et al., 2020; Wan et al., 2020).

The preparation of simulated gastric fluid (SGF) was as follows: 0.2 g of NaCl was dissolved in ultra-pure water, 0.45 g of pepsin (Aladdin, 1:15,000) and 0.032 g of rabbit gastric lipase (RGE25, 25 U/mg) were added. The solution was then adjusted to 100 mL with ultra-pure water and the pH adjusted to 3.0 with 1.0 mol/L HCl.

The preparation of simulated intestinal fluid (SIF) was as follows: 0.68 g of dipotassium hydrogen phosphate was dissolved in ultra-pure water, 0.12 g of bovine bile salt and 0.1 g of porcine pancreatin (Sigma-Aldrich, 30 U/mg) were added. The solution was then adjusted to 100 mL with ultra-pure water and the pH adjusted to 6.8 with 1.0 mol/L HCl.

For the stomach phase, 10 mL of freshly prepared emulsion was heated at 37 °C for 10 min, and 5 mL of SGF was added. The mixture was stirred at 37 °C for 30 min. The pH was maintained at 3.0 by adding 0.1 mol/L NaOH to neutralize the fatty acids released, and the added amount of NaOH at different times were recorded. For the small intestine phase, the pH of the sample from the stomach phase was adjusted to 6.8, and 10 mL of SIF was added. The mixture was stirred at 37 °C for 120 min. The pH value was maintained at 6.8 by adding 0.1 mol/L NaOH to neutralize the fatty acids released, and the added amount of NaOH at different times were recorded. The digested samples in the gastric and intestinal phases were collected at 30 and 150 min, respectively. After heated at 100 °C for 10 min to inactivate the enzyme, the samples were cooled immediately in an ice-water bath. The digestion of BCO-SF, PM and HMFS was performed in triplicate.

The percentage of fatty acid released was calculated by recording the volume of NaOH used to neutralize the fatty acid produced by the triglycerides (assuming 2 fatty acids released per triglyceride) (Equation 2):

$$Fatty\ acid\ released\,(\%) = (Co \times Vc \times M)\,/\,2m \times 100 \qquad (2)$$

Co: Concentration of NaOH solution (0.1 mol/L). Vc: Total volume of consumed NaOH solution (mL). M: Average molecular mass of sample (g/mol). m: Mass of sample in oil emulsion (g).

2.12 Measurements of droplet size and zeta-potential

The droplet size and zeta-potential of emulsion samples before and after digestion were determined by using a Zetasizer 2000 (Nano-ZS, Malvern Instruments, Worcestershire, UK). All measurements were performed three times at 25 °C.

2.13 Statistical analysis

Results were expressed as mean ± standard deviation (SD). Data were assessed using one-way analysis of variance (ANOVA), followed by Tukey's test with SPSS Statistics 22.0 Software. Figures were made by Origin 9.0 Software. $P < 0.05$ was considered statistically significant.

3 Results and discussion

3.1 Fractionation of basa catfish oil

After fractionation, the contents of sn-2 PA in BCO-SF and BCO-LF were 59.10 ± 0.18% and 33.90 ± 1.62% respectively (Table 1). The high content of sn-2 PA can ensure that the HMFS obtained by the reaction may still have a higher content of sn-2 PA. As shown in Figure 1, the melting temperature of BCO-SF (45.77 °C) was significantly higher than that of BCO-LF (10.51 °C) after fractionation which may be caused by the changes in the structure of triglycerides. Zou et al. (2016a) also reported a similar result.

3.2 Optimization of lipase-catalyzed transesterification conditions

Enzyme selection

Six commercial immobilized lipases were used to compare for their abilities to produce HMFS at their suitable temperatures.
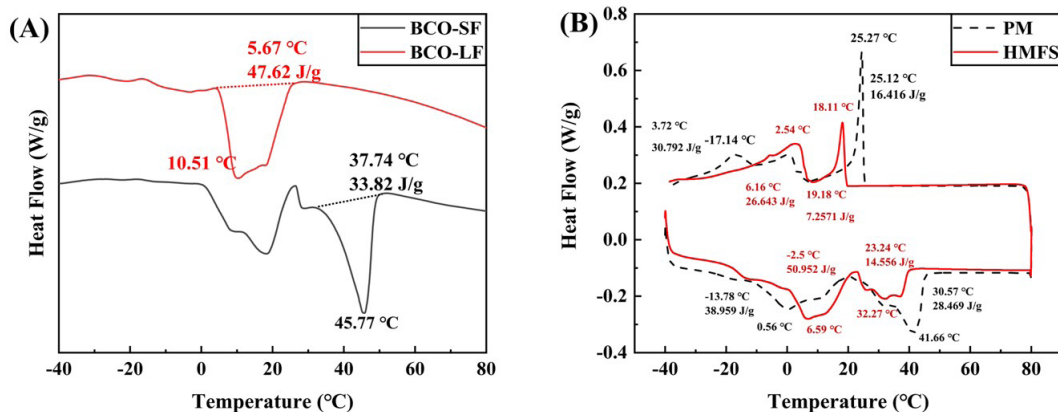
Figure 1. (A) Melting differential scanning calorimetry (DSC) profiles of BCO-SF (base catfish oil solid fraction) and BCO-LF (base catfish oil liquid fraction). (B) Melting and crystallization DSC profiles of PM (physical mixture) and HMFS (human milk fat substitute).

Table 1. Fatty acid composition and distribution of basa catfish oil solid fraction, basa catfish oil liquid fraction, CCSKO, LO, AO, MO, PM and HMFS.

Fatty acid	Basa catfish oil solid fraction Total	sn-2	Basa catfish oil liquid fraction Total	sn-2	CCSKO Total	sn-2	LO Total	sn-2	AO Total	sn-2	MO Total	sn-2	PM Total	sn-2	HMFS Total	sn-2
C8:0	0.23 ± 0.10[a]	0.09 ± 0.00	0.06 ± 0.00[b]	ND	0.62 ± 0.05	0.44 ± 0.03	ND	ND	ND	ND	ND	ND	0.22 ± 0.01	0.42 ± 0.03	0.33 ± 0.09	0.52 ± 0.07
C10:0	0.01 ± 0.00[A]	0.02 ± 0.00	0.07 ± 0.01[B]	ND	54.40 ± 0.09	61.02 ± 0.94	ND	ND	ND	ND	ND	ND	6.21 ± 0.49	8.48 ± 0.25	7.11 ± 0.44	8.35 ± 0.68
C12:0	0.13 ± 0.04[A]	0.17 ± 0.00[A]	0.53 ± 0.04[B]	1.33 ± 0.15[B]	41.08 ± 0.12	34.77 ± 0.69	ND	ND	ND	ND	ND	ND	4.50 ± 0.54	6.81 ± 0.11	4.48 ± 0.14	6.41 ± 0.94
C14:0	5.92 ± 0.03[a]	3.54 ± 0.03[a]	5.13 ± 0.08[B]	1.58 ± 0.73[b]	1.13 ± 0.01	0.77 ± 0.01	0.07 ± 0.00	ND	1.65 ± 0.05	ND	0.73 ± 0.01	ND	4.05 ± 0.18	3.44 ± 0.06	4.14 ± 0.05	3.24 ± 0.01
C16:0	46.24 ± 0.20[A]	59.10 ± 0.18[A]	33.70 ± 0.04[B]	33.90 ± 1.62[B]	0.41 ± 0.01	0.15 ± 0.02	7.79 ± 0.02	13.42 ± 0.26	51.41 ± 1.61	27.32 ± 0.65	11.48 ± 0.18	2.55 ± 0.41	32.25 ± 1.94	39.57 ± 1.52	32.70 ± 0.09	39.73 ± 1.46
C16:1	1.19 ± 0.00	1.26 ± 0.09	1.22 ± 0.02	0.65 ± 0.55	ND	0.09 ± 0.00	ND	ND	ND	ND	0.37 ± 0.01	ND	0.75 ± 0.04	ND	0.77 ± 0.01	ND
C18:0	10.16 ± 0.04[A]	6.09 ± 0.05	6.61 ± 0.11[B]	6.05 ± 0.32	0.21 ± 0.00	0.09 ± 0.00	3.91 ± 0.04	8.43 ± 0.06	3.01 ± 0.06	2.08 ± 0.07	6.96 ± 0.09	4.36 ± 0.48	7.55 ± 0.48	10.47 ± 0.23[A]	7.36 ± 0.02	9.00 ± 0.24[B]
C18:1	27.35 ± 0.11[A]	20.82 ± 0.13[A]	39.48 ± 0.24[B]	43.50 ± 2.13[B]	1.81 ± 0.02	0.97 ± 0.23	19.55 ± 0.13	28.02 ± 0.34	ND	ND	13.74 ± 0.3	22.07 ± 1.93	21.72 ± 1.12	11.51 ± 0.14[a]	20.35 ± 0.32	14.64 ± 1.87[b]
C18:2	6.75 ± 0.07[A]	7.78 ± 0.03[A]	10.52 ± 0.16[B]	12.99 ± 0.45[B]	0.32 ± 0.00	1.78 ± 0.05	15.56 ± 0.02	15.80 ± 0.19	ND	ND	6.06 ± 0.1	3.46 ± 0.28	7.47 ± 0.4	9.22 ± 0.31	7.60 ± 0.1	8.74 ± 1.05
C18:3n6	0.19 ± 0.02[A]	0.20 ± 0.00	0.31 ± 0.01[B]	ND	ND	ND	3.01 ± 0.02	ND	ND	ND	3.02 ± 0.02	2.16 ± 0.23	0.75 ± 0.04[A]	ND	0.62 ± 0.01[B]	ND
C18:3n3	0.28 ± 0.02[A]	0.56 ± 0.01	0.49 ± 0.08[b]	ND	ND	ND	50.12 ± 0.21	34.33 ± 0.44	ND	ND	ND	ND	10.93 ± 0.6	10.09 ± 0.11	11.43 ± 0.13	9.36 ± 0.84
C20:0	0.20 ± 0.01	ND	ND	ND	ND	ND	ND	ND	ND	ND	0.65 ± 0.01	ND	0.18 ± 0.01	ND	ND	ND
C20:1n9	0.76 ± 0.18	0.35 ± 0.01	0.78 ± 0.01	ND	ND	ND	ND	ND	ND	ND	ND	ND	0.42 ± 0.01	ND	0.40 ± 0.01	ND
C20:2	0.33 ± 0.00[A]	ND	0.50 ± 0.01[B]	ND	ND	ND	ND	ND	ND	ND	0.74 ± 0.00	ND	0.49 ± 0.3	ND	0.69 ± 0.16	ND
C20:3n6	0.25 ± 0.00[A]	ND	0.40 ± 0.00[B]	ND	ND	ND	ND	ND	ND	ND	4.52 ± 0.03	10.77 ± 0.59	0.27 ± 0.01	ND	ND	ND
C20:4n6	ND	ND	0.18 ± 0.00	ND	ND	ND	ND	ND	1.08 ± 0.04	2.45 ± 0.47	43.78 ± 0.35	54.63 ± 1.84	1.01 ± 0.05	ND	1.04 ± 0.01	ND
C22:0	ND	ND	ND	ND	ND	ND	ND	ND	8.56 ± 0.13	ND	2.12 ± 0.07	ND	ND	ND	ND	ND
C24:0	ND	ND	ND	ND	ND	ND	ND	ND	ND	ND	5.84 ± 0.17	ND	0.28 ± 0.01	ND	ND	ND
C22:6	ND	ND	ND	ND	ND	ND	ND	ND	34.29 ± 0.79	68.15 ± 1.89	ND	ND	0.96 ± 0.04[a]	ND	0.98 ± 0.03[b]	ND

The solid fraction and liquid fraction were divided after programmed temperature treatment of basa catfish oil at 80 °C for 40 min, followed by 30 °C for 24 h. CCSKO = *Cinnamomum camphora* seed kernel oil; LO = Linseed oil; AO = Algae oil; MO = Microbial oil. PM was the mixture oil with the BCO-SF, CCSKO, LO, AO and MO before the reaction; HMFS was synthesized with Lipozyme RM IM of 10 wt% and substrates of BCO-SF, CCSKO, LO, AO and MO at 60 °C for reaction time of 8 h. ND = no detected. Different letters denote significant different between basa catfish oil solid fraction and basa catfish oil liquid fraction, PM and HMFS (capital letter, $p < 0.01$; lowercase letter, $p < 0.05$).

Among them, Novozyme 435 and Lipozyme 435 are non-selective lipases, and the others are sn-1, 3 specific lipases (Yu et al., 2016). As shown in Figure 2 A, Lipozyme TL IM had the lowest STG yield (45.51 ± 1.27%), and there were no significant differences between NS 40086 (56.52 ± 1.34%), Lipozyme RM (58.86 ± 1.75%) and Lipozyme RM IM (57.62 ± 2.34%). However, both of them (Lipozyme TL IM, NS 40086, Lipozyme RM and Lipozyme RM IM) showed lower STG yields than Lipozyme 435 (64.82 ± 1.16%) and Novozyme 435 (67.30 ± 1.24%), which may be attributed to the non-selectivity of Novozym 435 and Lipozyme 435. The sn-2 PA content of the HMFS product catalyzed by Lipozyme 435 (33.75 ± 0.78%) was the lowest (Figure 2B). Therefore, taking the yield of STG and the content of sn-2 PA into consideration, Lipozyme RM was selected as the best lipase for the subsequent studies.

Optimization of reaction conditions

As shown in Figure 2, six different temperatures were used to assess the influence of temperature on the transesterification reaction. The yield of STG increased significantly (from 43.52 ± 0.54% to 58.83 ± 0.84%) when the temperature increased from 50 to 60 °C (Figure 2C), and the yield increased slightly with the further increase of reaction temperature. This may be because a suitable high temperature could reduce the viscosity of lipid mixture, and thus improve the transesterification rate between BCO-SF, CCSKO, LO, AO and MO. However, a higher temperature may denature the lipase, reducing the activity and half-life of the lipase. Besides, a higher temperature may lead to the oil peroxidation and affect the quality of lipid. Therefore, the optimum temperature was determined to be 60 °C and used for further studies. Furthermore, monitoring the time course in enzymatic reactions is useful for the determination of the optimal reaction time for obtaining the highest yield and minimizing the overall production cost. As shown in Figure 2D, the yield of STG increased significantly within the initial 8 h (from 29.43 ± 1.18% to 58.89 ± 0.61%), and then slightly decreased until 10 h. Based on the results, 8 h was chosen as the optimal reaction time to guarantee both better STG yield and efficiency.

The yield of STG increased from 31.12 ± 1.08% to 58.78 ± 1.03% when the enzyme amount increased from 2 to 10% (Figure 2E). However, when the enzyme amount was over 10%, there was a little reduction in STG yield. These results may be because a higher enzyme amount may lead to the lipase agglomeration and the diffusion of the substrates. Considering the yield of STG and the cost of enzyme, 10% (w/w total reactants) enzyme amount was chosen for the further transesterification reaction.

In summary, the results indicated the possibility of saving time and resources. Single-factor experiments could minimize the use of resources by reducing the reaction temperature (from 75 °C to 60 °C), enzyme load (from 14% to 10%) and time
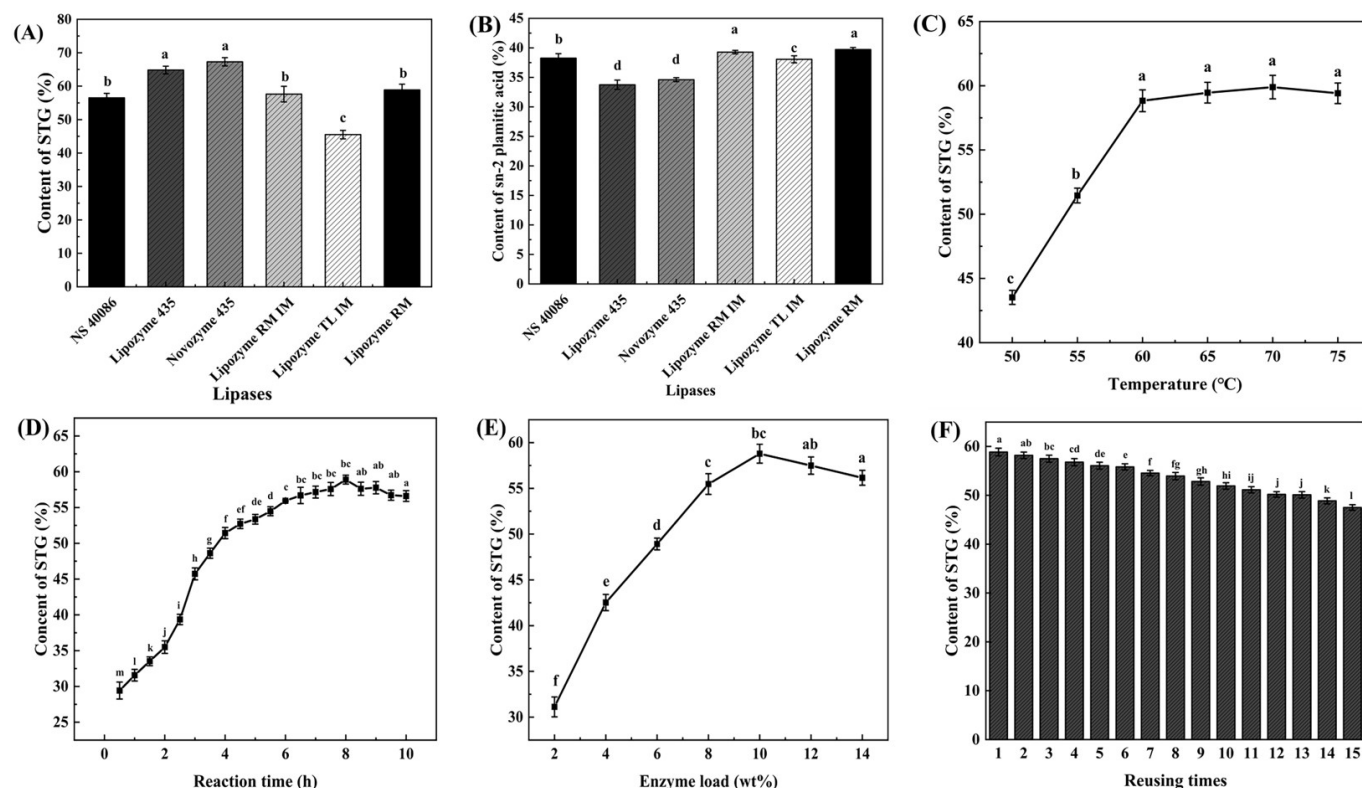
Figure 2. (A) The STG content in the reaction product by NS 40086, Lipozyme 435, Novozyme 435, Lipozyme RM IM, Lipozyme TL IM and Lipozyme RM. (B) The content of sn-2 palmitic acid in the reaction product by NS 40086, Lipozyme 435, Novozyme 435, Lipozyme RM IM, Lipozyme TL IM and Lipozyme RM. The effects of temperature (C), reaction time (D) and enzyme load (E) on the STG content in the reaction product using Lipozyme RM. (F) Reusability of Lipozyme RM in the interesterification under the optimal conditions. Different lowercase letters indicate significant differences ($p < 0.05$).

(from 10 h to 8 h), achieving the effect of energy conservation and emission reduction.

Reusability of the lipase

Considering the production cost, the reusability of an immobilized lipase is one of the most vital factors. During the repeated use of the lipase, its activity may be affected by the high temperature and agitation. The stability of Lipozyme RM was studied under the optimal conditions. The activity was assessed by the yield of STG. Figure 2F showed the reusability of Lipozyme RM under the above optimal reaction conditions. After 15 times reaction there was still approximately 80% (47.50 ± 0.58%) of the initial reaction yield (58.86 ± 0.78%). This result indicated that Lipozyme RM had excellent stability under the optimal reaction conditions. The result is basically consistent with a previous report (Yuan et al., 2020).

In the actual production of HMFS, Lipozyme RM can be reused more than 15 times, which means this not only can reduce the loss of enzyme in the production process and significantly reduce production costs, but also can reduce waste and protect the environment.

3.3 Fatty acid profile

As shown in Table 1, the major fatty acids of BCO-SF were PA (46.24 ± 0.20%) and O (27.35 ± 0.11%). It was worth mentioned that BCO-SF had the high content of sn-2 PA (59.10 ± 0.18%). The major fatty acids of CCSKO were MCFAs, including capric acid (54.40 ± 0.09%) and lauric acid (41.08 ± 0.12%). LO contained high levels of long-chain unsaturated fatty acids, including linoleic acid (15.56 ± 0.02%), oleic acid (19.55 ± 0.13%) and linolenic acid (50.12 ± 0.21%). MO contained high content

of ARA (43.78 ± 0.35%), and DHA (34.29 ± 0.79%) was mainly found in AO. There was no significant difference in fatty acid profiles between PM and HMFS. HMFS was composed of capric acid (7.11 ± 0.44%), lauric acid (4.48 ± 0.14%), oleic acid (20.35 ± 0.32%), linoleic acid (7.60 ± 0.1%), linolenic acid (11.43 ± 0.13%), ARA (1.04 ± 0.01%) and DHA (0.98 ± 0.03%). Moreover, the content of MCFAs accounted for about 10% of the total fatty acids, and HMFS had a relatively high content of sn-2 PA (39.73 ± 1.46%), which was similar to HMF (Wei et al., 2019). Therefore, HMFS can not only provide infants with nutrition from linoleic acid and linolenic acid, but may also supplement adequate ARA and DHA. These essential fatty acids are important for the growth and development of babies (Janssen & Kiliaan, 2014). MCFAs (Ca and La) can be rapidly hydrolyzed, which can provide sufficient energy for infants. La also plays an important role in regulating intestinal flora and improving digestion and resistance of infants (Nejrup et al., 2017). Yuan et al. (2020) only focused on the addition of MCFAs and the content of PA at the sn-2 position, and the content of sn-2 PA in the final product was only 30%. Wang et al. (2021) prepared a product with high sn-2 PA content (87%), but without MCFAs and essential fatty acids. Compared with these products, HMFS prepared in this study contained both FAs sn-2 PA. So HMFS from BCO-SF, CCSKO, LO, AO and MO through transesterification may be used as a new source of infant food lipids.

3.4 Triacylglycerol

The TAG species and compositions of PM were significantly changed after the enzymatic transesterification reaction (Figure 3 and Table 2). Indelicato et al. (2017) also reported a similar result. A total of 112 TAG species in PM were identified, and 38 original TAGs disappeared after

Table 2. Compositions of triacylglycerol in PM and HMFS.

PM					HMFS				
TAG	CN	DB	ECN		TAG	CN	DB	ECN	
Cy-Ca-La; Ca-Ca-Ca	30	0	30	0.24 ± 0.01					
Cy-La-La; Ca-Ca-La	32	0	32	5.42 ± 0.13					
					Cy-Ln-Et; Ca-Ln-Ln	46	6	34	1.14 ± 0.02
Ca-La-La; Ca-Ca-M; Cy-Ca-P	34	0	34	7.96 ± 0.21					
Ln-Ln-Ln	54	9	36	4.22 ± 0.14	Ln-Ln-Ln; M-Ln-DHA	54	9	36	2.36 ± 0.07
					L-L-DHA; P-ARA-DHA; Po-Et-DHA; O-Ln-DHA	58	10	38	6.58 ± 0.64
Po-ARA-ARA; Po-L-DHA; L-Ln-ARA	56	9	38	5.77 ± 0.15					
Po-Ln-ARA; L-Ln-Ln; M-ARA-ARA; M-L-DHA	54	8	38		Po-Ln-ARA; L-Ln-Ln	54	8	38	
					Cy-Ed-Et; Ca-Ln-Ed; Cy-Eo-ARA; Ca-O-ARA; La-Po-ARA	48	5	38	
					Cy-O-Et; Ca-O-Ln; Cy-Ln-Eo; Ca-O-Ln; La-Po-Ln; Ca-L-L; Ca-P-ARA; Ca-Po-Et	46	4	38	
					Co-Ln-E; Cy-S-Ln; Ca-P-Ln; La-M-Ln; Cy-P-Et; Ca-M-Et; Ca-Po-L	44	3	38	

Equivalent carbon number (ECN) = CN-2DB.CN is the number of carbon atoms in the acyl residue of TAG and DB is the number of double bonds of fatty acids forming TAG. Abbreviations of fatty acids: Cy = C8:0; Ca = C10:0; La = C12:0; M = C14:0; P = C16:0; Po = C16:1; S = C18:0; O = C18:1; L =18:2; Ln = C18:3; E = C20:0; Eo = C20:1; Ed = C20:2; Et = C20:3; ARA = C20:4; DHA = C22:6; Lg = C24:0.

Table 2. Continued...

PM					HMFS				
TAG	CN	DB	ECN		TAG	CN	DB	ECN	
L-Et-ARA; P-Et-DHA	58	9	40	2.86 ± 0.24					7.20 ± 0.32
Po-L-ARA; P-Ln-ARA; Po-Ln-Et; O-Ln-Ln; L-L-Ln; P-Po-DHA; M-Et-ARA; M-O-DHA	54	7	40		M-Et-ARA; P-Ln-ARA; Po-L-ARA; L-L-Ln; Po-Ln-Et; O-Ln-Ln	54	7	40	
M-Ln-Et; P-Ln-Ln; Po-L-Ln; M-P-DHA; M-L-ARA	52	6	40		M-Ln-Et; P-Ln-Ln; Po-L-Ln; La-Et-Et; La-S-DHA; La-Ed-ARA	52	6	40	
					La-L-L; La-P-ARA; La-Po-Et; La-O-Ln; Cy-Eo-Et; Ca-O-Et; M-M-ARA; Cy-E-ARA; Ca-S-ARA	48	4	40	
					Co-E-Et; Cy-S-Et; Ca-P-Et; La-M-Et; Cy-O-Ed; Ca-O-L; La-P-Ln; La-Po-L; M-M-Ln; Cy-Ln-E; Ca-S-Ln	46	3	40	
					O-O-DHA; P-Ed-DHA; Po-Eo-DHA; S-L-DHA	58	8	42	26.84 ± 0.48
P-Ln-Et; Po-Ln-Ed; S-Ln-Ln; O-L-Ln; Po-O-ARA; Po-L-Et; M-Ed-ARA; P-L-ARA; M-Et-Et; M-S-DHA	54	6	42	3.26 ± 0.07	M-Ed-ARA; P-L-ARA; Po-O-ARA; P-Ln-Et; Po-Ln-Ed; S-Ln-Ln; O-L-Ln	54	6	42	
Po-L-L; P-Po-ARA; Po-Po-Et; Po-O-Ln; M-O-ARA; M-Ln-Ed; P-L-Ln; M-L-Et	52	5	42		M-Ln-Ed; P-L-Ln; Po-O-Ln; La-Ed-Et; La-Eo-ARA; M-O-ARA; P-Po-ARA	52	5	42	
					Ca-E-ARA; La-S-ARA; M-P-ARA; La-O-Et; M-O-Ln; La-Ln-Eo; P-Po-Ln	50	4	42	
					La-P-Et; M-P-Ln; M-M-Et; Cy-E-Et; Ca-S-Et; Ca-Ln-E; La-S-Ln; M-P-Ln; Ca-O-Ed; La-O-L	48	3	42	
					M-M-L; Cy-L-E; Ca-S-L; La-P-L; Ca-P-Ed; La-M-Ed; La-Po-O; Ca-O-O; Ca-Po-Eo; Ca-S-L	46	2	42	
P-L-Et; Po-L-Ed; S-L-Ln; O-L-L; Po-S-ARA; Po-O-Et; Po-Ln-Eo; P-O-ARA; O-O-Ln; M-Ed-Et; P-Ln-Ed; M-Eo-ARA	54	5	44	15.32 ± 0.41	M-Eo-ARA; P-O-ARA; Po-S-ARA; P-L-Et; Po-L-Ed; S-L-Ln; O-L-L; Po-O-Et; O-O-Ln; M-Ed-Et; P-Ln-Ed	54	5	44	21.09 ± 0.51
P-P-ARA; M-S-ARA; P-L-L; P-Po-Et; P-O-Ln; M-L-Ed; Po-O-L; M-O-Et; M-Ln-Eo; Po-S-Ln	52	4	44		P-P-ARA; La-E-ARA; M-S-ARA; M-L-Ed; P-L-L; Po-O-L; P-Po-Et; P-O-Ln; M-Ln-Eo; Po-S-Ln; Po-Po-Ed; La-Ed-Ed; M-O-Et	52	4	44	
					Ca-E-Et; La-S-Et; M-P-Et; P-P-Ln; La-Ln-E; M-S-Ln; Po-P-L	50	3	44	
					P-Ed-Et; Po-Ed-Ed; S-Ln-Ed; O-L-Ed	56	5	46	10.18 ± 0.77
P-O-Et; Po-O-Ed; S-O-Ln; O-O-L; M-Ed-Ed; P-L-Ed; Po-L-Eo; S-L-L; M-Eo-Et; Po-S-Et	54	4	46	23.86 ± 0.47	Ca-Lg-ARA; M-E-ARA; P-S-ARA; P-O-Et; Po-O-Ed; S-O-Ln; O-O-L; M-Ed-Ed; P-L-Ed; M-Eo-Et; Po-S-Et	54	4	46	
M-L-Eo; P-O-L; Po-S-L; P-P-Et; P-Po-Ed; P-S-Ln; M-O-Ed; Po-O-O; Po-Po-Eo	52	3	46		P-P-Et; La-E-Et; M-S-Et; M-O-Ed; P-O-L; Po-O-O; P-Po-Ed; P-S-Ln; M-L-Eo; Po-S-L	52	3	46	
					La-O-Eo; M-O-O; P-Po-O	50	2	46	
					Ca-O-E; La-S-O; M-P-O; La-P-Eo; M-P-O; P-P-Po	48	1	46	
O-O-O; P-O-Ed; Po-O-Eo; S-O-L; M-Eo-Ed; Po-S-Ed	54	3	48	21.06 ± 0.75	Ca-Lg-Et; M-E-Et; P-S-Et; O-O-O; P-O-Ed; Po-O-Eo; S-O-L; M-Eo-Ed; Po-S-Ed	54	3	48	16.40 ± 0.41
M-O-Eo; P-O-O; Po-S-O; P-P-Ed; P-Po-Eo; P-S-L	52	2	48		P-P-Ed; La-E-Ed; M-S-Ed; M-O-Eo; P-O-O; Po-S-O	52	2	48	
P-P-O; M-S-O; M-P-Eo; P-Po-S	50	1	48		P-P-O; La-O-E; M-S-O; M-P-Eo; P-Po-S	50	1	48	

Equivalent carbon number (ECN) = CN-2DB.CN is the number of carbon atoms in the acyl residue of TAG and DB is the number of double bonds of fatty acids forming TAG. Abbreviations of fatty acids: Cy = C8:0; Ca = C10:0; La = C12:0; M = C14:0; P = C16:0; Po = C16:1; S = C18:0; O = C18:1; L =18:2; Ln = C18:3; E = C20:0; Eo = C20:1; Ed = C20:2; Et = C20:3; ARA = C20:4; DHA = C22:6; Lg = C24:0.

Table 2. Continued...

PM					HMFS				
TAG	CN	DB	ECN		TAG	CN	DB	ECN	
					P-Eo-Ed; Po-E-Ed; S-O-Ed	56	3	50	7.63 ± 0.68
P-O-Eo; Po-O-E; S-O-O	54	2	50	10.04 ± 0.33	P-O-Eo; Po-O-E; S-O-O; M-Eo-Eo; Po-S-Eo	54	2	50	
M-S-Eo; P-S-O; Po-S-S; P-P-Eo; P-Po-E; D-D-O; M-S-Eo	52	1	50		M-S-Eo; P-S-O; Po-S-S; Ca-O-Lg; M-O-E; P-P-Eo; La-E-Eo	52	1	50	
					Ca-P-Lg; M-P-E; P-P-S	50	0	50	
					Ca-Lg-Eo; M-E-Eo; P-S-Eo; S-S-O; La-O-Lg; P-O-E	54	1	52	0.58 ± 0.05

Equivalent carbon number (ECN) = CN-2DB.CN is the number of carbon atoms in the acyl residue of TAG and DB is the number of double bonds of fatty acids forming TAG. Abbreviations of fatty acids: Cy = C8:0; Ca = C10:0; La = C12:0; M = C14:0; P = C16:0; Po = C16:1; S = C18:0; O = C18:1; L =18:2; Ln = C18:3; E = C20:0; Eo = C20:1; Ed = C20:2; Et = C20:3; ARA = C20:4; DHA = C22:6; Lg = C24:0.
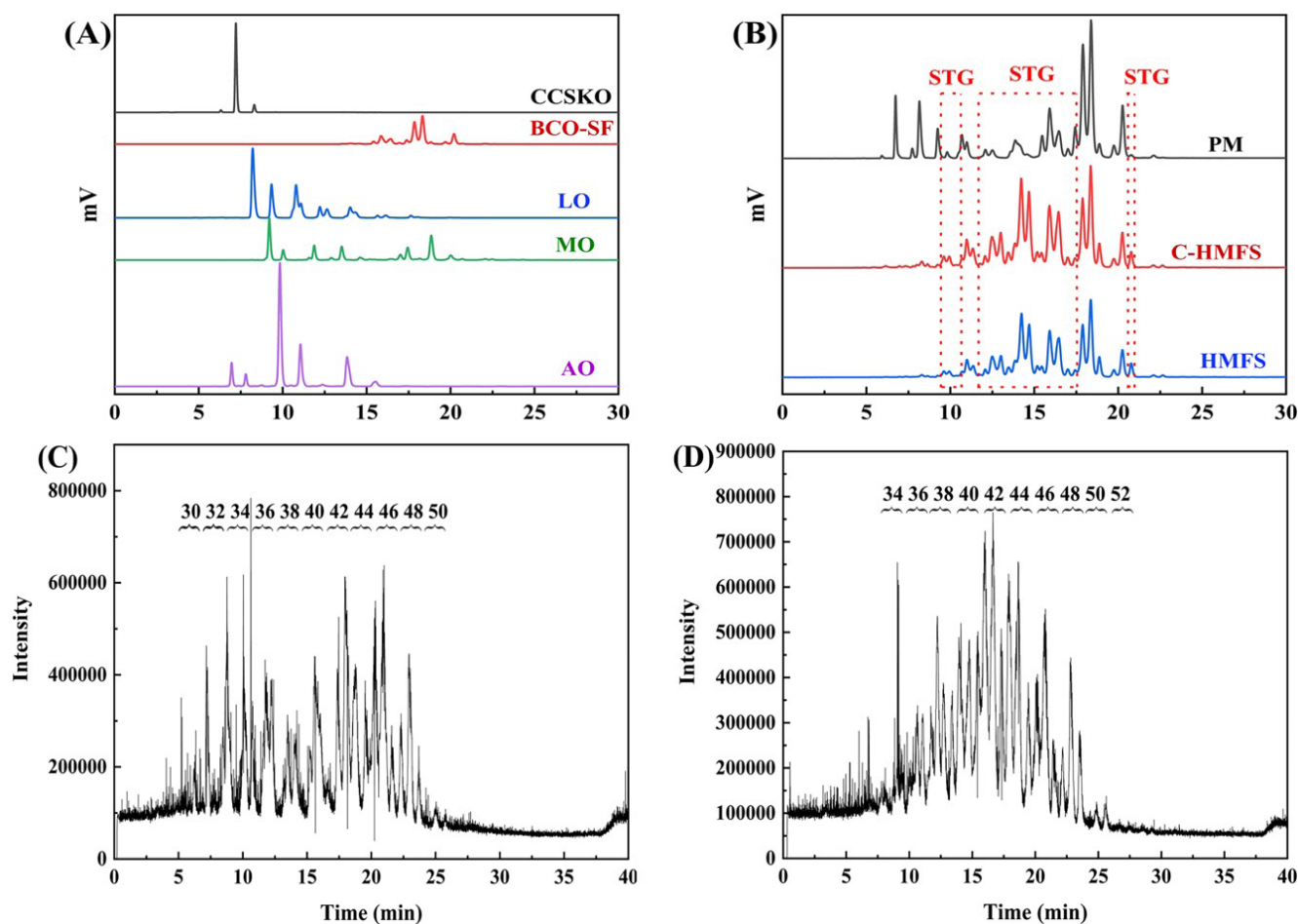
Figure 3. (A) High performance liquid chromatography (HPLC) chromatograms of TAG species of CCSKO, BCO-SF, LO, MO and AO. (B) HPLC chromatograms of TAG species of PM, C-HMFS and HMFS (human milk fat substitute). (C) and (D) Chromatograms of TAGs in PM and HMFS obtained by Hybrid Quadrupole-TOF Mass Spectrometer.

transesterification, such as Cy-Ca-La, Ln-Ln-Ln, L-Ln-ARA, L-Et-ARA and M-S-DHA. Interestingly, the HMFS contained 216 triglycerides, including 142 new triglycerides, such as P-ARA-DHA, Ca-P-ARA, Ca-P-Ln, La-P-ARA, La-P-L, P-P-Ln and P-O-ARA which were found in HMF. The structures of the newly generated triglycerides may not only ensure that PA is located at the sn-2 position of the glycerol skeleton, but also ensure that the MCFAs and essential fatty acids are located at the sn-1,3 positions of the glycerol skeleton. The unique TAG structures of HMFS may allow infants to better absorb and utilize fatty acids. These results indicated that enzymatic transesterification has taken place, and the HMFS with a high yield of STG was obtained. It can be also concluded that HMFS was rich in new medium and long chain triglycerides with Ca, La, L, Ln, ARA and DHA, which may be beneficial to the digestion and absorption of infants.

According to a previous study (Wei et al., 2019), human milk contains more than 50 fatty acids and 400 TAGs. The HMFS product in this study included 18 fatty acids and 216 TAG and was closer to HMF. The most abundant TAGs containing MCFAs in human milk were Ca-L-L, La-P-L, La-O-L, Ca-P-Ln, La-L-L and Ca-O-O. However, the TAGs containing La in HMFS have been rarely reported, and the TAGs were mainly composed of Ca (Korma et al., 2018). It was also reported that the TAGs in HMFS only contained LCFAs, such as P-O-L, P-O-L, P-P-O, P-P-ARA, P-Ln-ARA, O-O-DHA and P-O-O (Yuan et al., 2020). Therefore, the HMFS product obtained in this study was more closer to HMF and more suitable for infant food in the respect of FA and TAG compositions.

3.5 FT-IR spectra

The FT-IR spectra of the samples before and after transesterification are shown in Figure 4A-B. The peaks near 2920 cm^{-1} and 2850 cm^{-1} are related to the stretching vibrations of CH$_3$ and CH$_2$. The characteristic peaks of C=O are related to ester bonds near 1740 cm^{-1}. The peaks near 1464 cm^{-1} are related to CH. The peaks around 1150 cm^{-1} and 1090 cm^{-1} correspond to the stretching vibration absorption peaks of C-O-C. It was found that there were no significant changes in the functional groups of the samples before and after transesterification. Except for an obvious -OH group (3380 cm^{-1}) found in the C-HMFS, the remaining peak positions were basically the same as the others, indicating that the functional groups on the triglycerides were not changed during the transesterification process. The results were similar to a previous report (Zhang et al., 2019). Although free fatty acids were produced during transesterification, no trans fatty acids (996 cm^{-1}) were produced. It can be concluded that the transesterification reaction is green and safe.

3.6 Thermal behavior

The PM had a melting peak at 41.66 °C. After transesterification, a main melting point peak of HMFS at 32.27 °C and one shoulder peak at 6.59 °C were observed (Figure 1B). As shown in the crystallization curve, PM exhibited a crystal peak at 25.27 °C.

After transesterification, the crystallization point peak of HMFS shifted to the left, with the main crystallization peak at 18.11 °C and one shoulder peak at 2.54 °C. These results indicated that the melting point and crystallization capacity of HMFS were significantly lower than those of PM. The lower melting point of HMFS than human body temperature (37 °C) indicated that HMFS may be more conducive to body absorption (Korma et al., 2018).

3.7 In vitro digestion

In the course of the digestion process, the droplet size and zeta potential of the emulsion before and after digestion were measured (Figure 5A-B). For the emulsions freshly prepared, the zeta potential of PM and HMFS were -70.88 ± 1.79 mV and -74.56 ± 0.53 mV, respectively, and the droplet size of PM and HMFS were 393.48 ± 14.13 nm and 368.37 ± 25.71 nm, respectively. HMFS showed higher droplet size and lower zeta potential than those of PM, indicating that the emulsion prepared by HMFS was more unstable than that prepared by PM. Similar phenomenon was also observed in gastric and intestinal phases. After the two phases of digestion, the particle size of PM and HMFS were significantly increased, which may be related to the increase in the affinity of bile salts and droplets. Moreover, the absolute value of zeta potential of PM and HMFS were decreased after the two phases of digestion. This may be because during the digestion process, pancreatin destroyed the structure of the emulsion droplets, reducing the negative charge on the surface of the droplets and reducing the electrostatic repulsion between the particles, which ultimately led to an increased zeta potential of the entire emulsion system. However, as shown in Figure 5C, PM had the higher digestibility than HMFS in the process of gastric digestion. This is directly proportional to its particle size. The smaller particle size allows the fat to better contact with the digestive juices, and is the more conducive to digestion and decomposition of fat which is related to the specific surface area of the droplets in the emulsion. Furthermore, in the process of intestinal digestion, HMFS exhibited significantly higher fatty acid release rate than PM, with the final values of 66.82 ± 2.06% and 52.76 ± 1.41% for HMFS and PM, respectively.
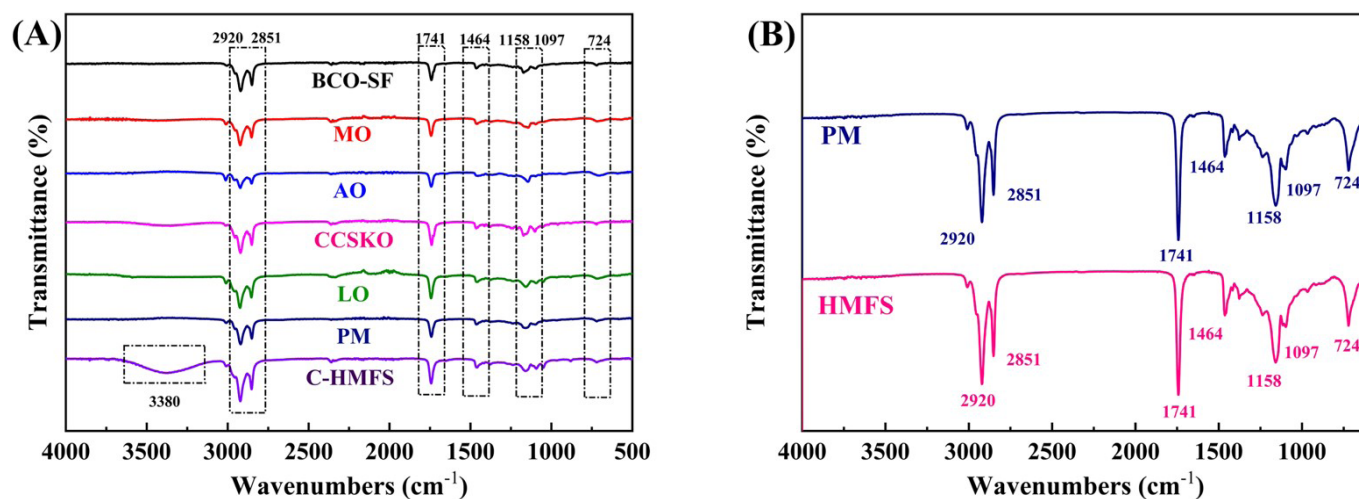
Figure 4. (A) Fourier transform infrared (FT-IR) spectra of BCO-SF, MO, AO, CCSKO, LO, PM and C-HMFS. (B) FT-IR spectra of PM and HMFS.
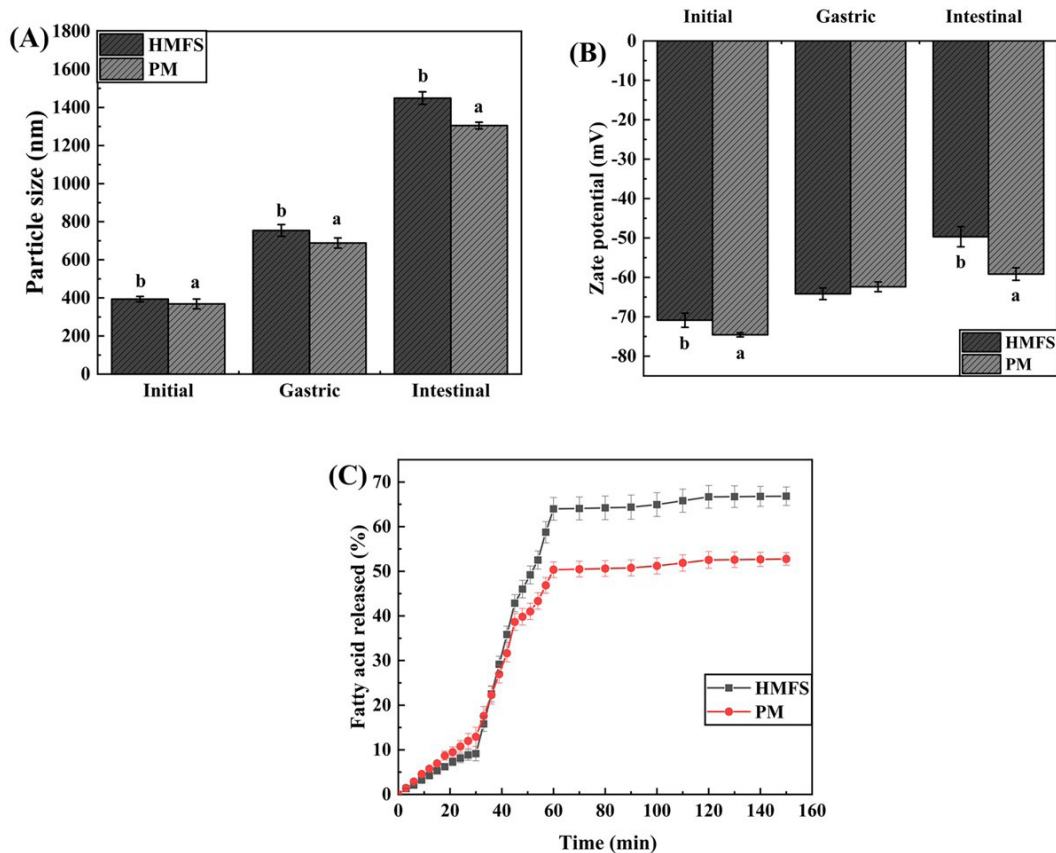
Figure 5. (A) and (B) Mean particle size and zeta of emulsion samples before (initial) and after simulated digestion. (C) Fatty acid released from emulsions during simulated gastric and intestinal digestion. Different lowercase letters indicate significant differences ($p < 0.05$) from different emulsions within the same digestion phase.

These results may be related to their melting points and the sn-1,3-specific lipase in the intestinal lipase. The lipid with higher content of sn-2 PA may have better affinity and digestibility in the intestinal digestive juice. The lower melting point of HMFS may allow the fat to better contact with the digestive juices, which is the more conducive to digestion and decomposition of fat (Wan et al., 2020). PM contains more high melting point long chain triglycerides, which may lead to insufficient contact between PM and digestive fluid.

The results of *in vitro* digestion have shown that after transesterification, HMFS had higher *in vitro* digestion effect than PM. This may be because HMFS not only had a higher content of sn-2 PA, but also had a suitable melting point for the human body.

4 Conclusions

In this study, HMFS was successfully produced in a solvent-free system by lipase-catalyzed transesterification of BCO-SF, CCSKO, LO, AO and MO using Lipozyme RM as a biocatalyst. Under the optimal reaction conditions (reaction temperature at 60 °C, reaction time of 8 h and enzyme load of 10%), HMFS with the highest STG and sn-2 PA content was prepared. Lipozyme RM can be reused for 15 times with the remaining activity of over 80%, showing high application potential. After

transesterification reaction, the melting point of HMFS was significantly lower than that of PM. Compared with PM, HMFS showed better *in vitro* digestibility, manifested by higher fatty acid release rate. These results suggested that HMFS may have great development potential in the future of infant food.

References

Colombo, J., Shaddy, D. J., Kerling, E. H., Gustafson, K. M., & Carlson, S. E. (2017). Docosahexaenoic acid (DHA) and arachidonic acid (ARA) balance in developmental outcomes. *Prostaglandins, Leukotrienes,*

and Essential Fatty Acids, 121, 52-56. http://dx.doi.org/10.1016/j.plefa.2017.05.005. PMid:28651697.

Fu, J., Wang, B., Gong, D., Zeng, C., Jiang, Y., & Zeng, Z. (2015). Camphor tree seed kernel oil reduces body fat deposition and improves blood lipids in rats. *Journal of Food Science*, 80(8), H1912-H1917. http://dx.doi.org/10.1111/1750-3841.12943. PMid:26130050.

Fu, J., Zeng, C., Zeng, Z., Wang, B., Wen, X., Yu, P., & Gong, D. (2016). Cinnamomum camphora seed kernel oil improves lipid metabolism and enhances beta3-adrenergic receptor expression in diet-induced obese rats. *Lipids*, 51(6), 693-702. http://dx.doi.org/10.1007/s11745-016-4147-8. PMid:27068065.

Gahroui, M. R., Hojjatoleslamy, M., Kiani, H., & Molavi, H. (2022). Feasibility study and optimization of infant formula production using a mixture of camel milk and cow milk. *Food Science and Technology*, 42, e56720. http://dx.doi.org/10.1590/fst.56720.

Indelicato, S., Bongiorno, D., Pitonzo, R., Stefano, V., Calabrese, V., Indelicato, S., & Avellone, G. (2017). Triacylglycerols in edible oils: determination, characterization, quantitation, chemometric approach and evaluation of adulterations. *Journal of Chromatography A*, 1515, 1-16. http://dx.doi.org/10.1016/j.chroma.2017.08.002. PMid:28801042.

Janssen, C. I., & Kiliaan, A. J. (2014). Long-chain polyunsaturated fatty acids (LCPUFA) from genesis to senescence: the influence of LCPUFA on neural development, aging, and neurodegeneration. *Progress in Lipid Research*, 53, 1-17. http://dx.doi.org/10.1016/j.plipres.2013.10.002. PMid:24334113.

Korma, S. A., Zou, X., Ali, A. H., Abed, S. M., Jin, Q., & Wang, X. (2018). Preparation of structured lipids enriched with medium- and long-chain triacylglycerols by enzymatic interesterification for infant formula. *Food and Bioproducts Processing*, 107, 121-130. http://dx.doi.org/10.1016/j.fbp.2017.11.006.

MacHate, D. J., Candido, C. J., Inada, A. C., Franco, B. C., Carvalho, I. R. A., Oliveira, L. C. S., Cortes, M. R., Caires, A. R. L., Silva, R. H., Hiane, P. A., Bogo, D., Lima, N. V., Nascimento, V. A., Guimarães, R. C. A., & Pott, A. (2020). Fatty acid profile and physicochemical, optical and thermal characteristics of Campomanesia adamantium (Cambess.) O. Berg seed oil. *Food Science and Technology*, 40(Suppl. 2), 538-544. http://dx.doi.org/10.1590/fst.32719.

Nejrup, R. G., Licht, T. R., & Hellgren, L. I. (2017). Fatty acid composition and phospholipid types used in infant formulas modifies the establishment of human gut bacteria in germ-free mice. *Scientific Reports*, 7(1), 3975. http://dx.doi.org/10.1038/s41598-017-04298-0. PMid:28638093.

Souza, M. W. S., Lopes, E. S. O., Cosenza, G. P., Alvarenga, V. O., Labanca, R. A., Araújo, R. L. B., & Lacerda, I. C. A. (2020). Effect of inulin, medium-chain triglycerides and whey protein isolate on stability and in vitro digestibility of enteral nutrition formulas. *Food Science and Technology*, 40(4), 854-863. http://dx.doi.org/10.1590/fst.23619.

Sun, C., Wei, W., Su, H., Zou, X., & Wang, X. (2018). Evaluation of sn-2 fatty acid composition in commercial infant formulas on the Chinese market: a comparative study based on fat source and stage. *Food Chemistry*, 242, 29-36. http://dx.doi.org/10.1016/j.foodchem.2017.09.005. PMid:29037692.

Uncu, O., Ozen, B., & Tokatli, F. (2019). Use of FTIR and UV-visible spectroscopy in determination of chemical characteristics of olive oils. *Talanta*, 201, 65-73. http://dx.doi.org/10.1016/j.talanta.2019.03.116. PMid:31122462.

Wan, L., Li, L., Harro, J. M., Hoag, S. W., Li, B., Zhang, X., & Shirtliff, M. E. (2020). In vitro gastrointestinal digestion of palm olein and palm stearin-in-water emulsions with different physical states and fat contents. *Journal of Agricultural and Food Chemistry*, 68(26), 7062-7071. http://dx.doi.org/10.1021/acs.jafc.0c00212. PMid:32496800.

Wang, X., Huang, Z., Hua, L., Zou, F., Cheng, X., & Wang, X. (2021). Preparation of human milk fat substitutes similar to human milk fat by enzymatic acidolysis and physical blending. *Lebensmittel-Wissenschaft + Technologie*, 140, 110818. http://dx.doi.org/10.1016/j.lwt.2020.110818.

Wei, W., Jin, Q., & Wang, X. (2019). Human milk fat substitutes: past achievements and current trends. *Progress in Lipid Research*, 74, 69-86. http://dx.doi.org/10.1016/j.plipres.2019.02.001. PMid:30796946.

Yu, X. W., Xu, Y., & Xiao, R. (2016). Lipases from the genus Rhizopus: characteristics, expression, protein engineering and application. *Progress in Lipid Research*, 64, 57-68. http://dx.doi.org/10.1016/j.plipres.2016.08.001. PMid:27497512.

Yuan, T., Wei, W., Wang, X., & Jin, Q. (2020). Biosynthesis of structured lipids enriched with medium and long-chain triacylglycerols for human milk fat substitute. *Lebensmittel-Wissenschaft + Technologie*, 128, 109255. http://dx.doi.org/10.1016/j.lwt.2020.109255.

Yuan, T., Zhang, H., Wang, X., Yu, R., Zhou, Q., Wei, W., Wang, X., & Jin, Q. (2019). Triacylglycerol containing medium-chain fatty acids (MCFA-TAG): the gap between human milk and infant formulas. *International Dairy Journal*, 99, 104545. http://dx.doi.org/10.1016/j.idairyj.2019.104545.

Zhang, Z., Lee, W. J., & Wang, Y. (2021). Evaluation of enzymatic interesterification in structured triacylglycerols preparation: a concise review and prospect. *Critical Reviews in Food Science and Nutrition*, 61(19), 3145-3159. http://dx.doi.org/10.1080/10408398.2020.1793725. PMid:32696657.

Zhang, Z., Ye, J., Fei, T., Ma, X., Xie, X., Huang, H., & Wang, Y. (2019). Interesterification of rice bran wax and palm olein catalyzed by lipase: crystallization behaviours and characterization. *Food Chemistry*, 286, 29-37. http://dx.doi.org/10.1016/j.foodchem.2019.01.192. PMid:30827609.

Zhao, B., Gong, H., Li, H., Zhang, Y., Deng, J., & Chen, Z. (2019). Fatty acid, triacylglycerol and unsaponifiable matters profiles and physicochemical properties of Chinese evening primrose oil. *Journal of Oleo Science*, 68(8), 719-728. http://dx.doi.org/10.5650/jos.ess19091. PMid:31292343.

Zou, X., Jin, Q., Guo, Z., Huang, J., Xu, X., & Wang, X. (2016a). Preparation of 1, 3-dioleoyl-2-palmitoylglycerol-rich structured lipids from basa catfish oil: combination of fractionation and enzymatic acidolysis. *European Journal of Lipid Science and Technology*, 118(5), 708-715. http://dx.doi.org/10.1002/ejlt.201500226.

Zou, X., Jin, Q., Guo, Z., Xu, X., & Wang, X. (2016b). Preparation of human milk fat substitutes from basa catfish oil: combination of enzymatic acidolysis and modeled blending. *European Journal of Lipid Science and Technology*, 118(11), 1702-1711. http://dx.doi.org/10.1002/ejlt.201500591.

Zuin, J. C., Gandra, R. L. P., Ribeiro, A. P. B., Ract, J. N. R., Macedo, J. A., & Macedo, G. A. (2022). Comparing chemical and enzymatic synthesis of rich behenic lipids products: technological and nutritional potential. *Food Science and Technology*, 42, e105821. Ahead of print.

Abbreviations

AO: algae oil. APCI: atmospheric pressure chemical ionization. ARA: arachidonic acid. BCO: basa catfish oil. BCO-SF: basa catfish oil solid fraction. Ca: capric acid. CCSKO: *Cinnamomum camphora* seed kernel oil. DHA: docosahexaenoic acid. ELSD: evaporative light scanning detector. FAMEs: fatty acid methyl ester. FID: flame ionization detector. FT-IR: Fourier transform infrared. GC: gas chromatography. HMF: human milk fat. HMFS: human milk fat substitute. L: linoleic acid. La: lauric acid. LCFAs: long chain fatty acids. LC-MS/MS: liquid chromatography-mass spectrometry. Ln: linolenic acid. LO: linseed oil. MCFAs: medium chain fatty acids. MO: microbial oil. O: oleic acid. OPL: 1-oleoyl-2-palmitoyl-3-linoleoylglycerol. OPO: 1,3-dioleoyl-2-palmitoylglycerol. PA: palmitic acid. PM: physical mixture. RP-HPLC: reversed-phase high performance liquid chromatography. SGF: simulated gastric fluid. SIF: simulated intestinal fluid. STG: structured triglycerides. TAG: triglycerides.